ChemComm

Accepted Manuscript

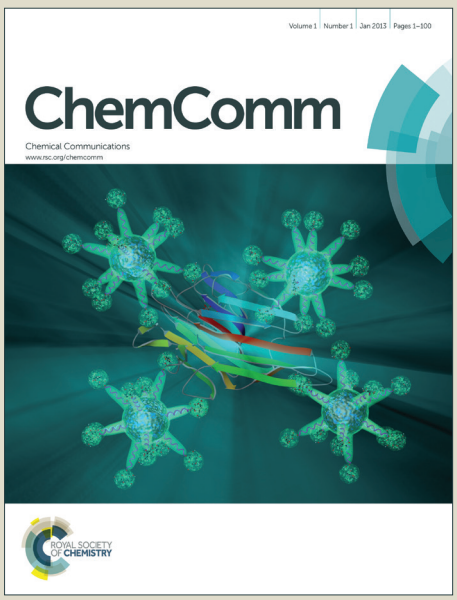

ROYAL SOCIETY OF CHEMISTRY

www.rsc.org/chemcomm

Cite this: DOI: 10.1039/c0xx00000x

www.rsc.org/xxxxxx

ARTICLE TYPE

Bio-catalytic Driven Janus Mesoporous Silica Cluster Motor with Magnetic Guidance

Xing Ma,[a] and Samuel Sanchez*[a]

Received (in XXX, XXX) Xth XXXXXXXXX 20XX, Accepted Xth XXXXXXXXX 20XX

DOI: 10.1039/b000000x

A bio-catalytic Janus motor based on mesoporous silica cluster (JMSC) is fabricated. Chemically conjugated catalase triggers decomposition of H_2O_2 to produce driving force by bubble propulsion, while metallic (Ni) coating layer allows for magnetic guidance on the motor. The JMSC motor can act as delivery vehicle with cargo loading inside its mesopores.

Janus structure has been employed to fabricate micro/nano motors (MNM),[1, 2] since distinguished surface properties of the two "faces" can produce a "net force" for the movement of Janus motors, such as catalytic reaction induced electrolyte/ionic self-diffusiophoresis,[3-7] bubble propulsion,[8-10] or neutral self-diffusiophoresis.[11, 12] At present, most Janus motors are mainly fabricated with solid spheres, like silica (SiO_2)[12] and polystyrene (PS) particles.[3, 11, 13] The rigid property of such motors limits their delivery capability, since cargos can only be loaded on Janus particles' outside surface. Furthermore, requirement of catalytic sites on motors' surface further minimizes cargo loading capability. Thus, the use of rigid Janus motors is limited as effective delivery vehicles. Mesoporous silica nanoparticles (MSNPs) have been widely investigated as catalyst support[14, 15] and drug/gene delivery carriers,[16, 17] in virtue of their unique structure, including tunable size, high surface area, uniform pore size and high pore volume,[18, 19] which allows for cargo molecules loading in large quantity.[20] So, it is of great interest to fabricate Janus motors with mesoporous silica materials,[21] considering their excellent capability of cargo loading and delivery.

As an important mechanism, bubble propulsion has been utilized to provide driving forces for micro/nano motors (MNM).[9, 22-24] Continuous production of bubbles is essential for the motors' movement by bubble propulsion mechanism. For example, in the case of micro-tube based jets, the internal catalytic metal platinum (Pt) layer can decompose H_2O_2 and bubbles are formed inside the micro-sized channels to provide the driving force for the jets movement.[24-26] However, for Janus particles based motors, bubbles can hardly form on the smooth surface of spherical particles, and usually a rough surface with small cavities is preferred for bubbles generation.[10, 27] During classic "sol-gel" synthesis of MSNPs by using NaOH as catalyst, it is a great challenge to obtain completely mono-dispersed MSNPs and considerable mesoporous silica cluster (MSC) presents due to "unwanted" aggregations.[28, 29] However, the other side of the coin is that small cavities or narrow gaps between aggregated MSNPs in these MSC might be able to serve as a rough surface and provide ideal nucleation sites for the bubble generation and local accumulation, thus driving the movement of motors by bubble propulsion.

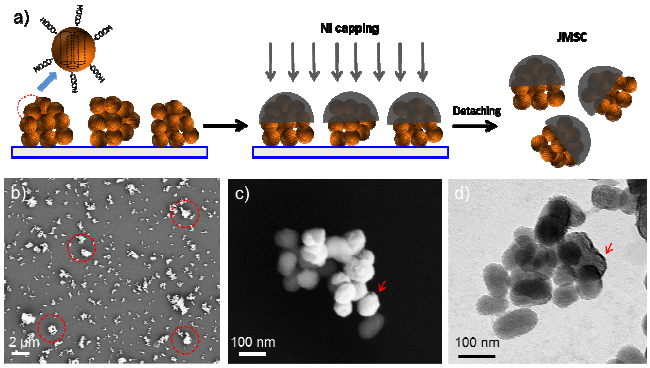

Figure 1. a) Schematic illustration of Janus mesoporous silica cluster (JMSC) fabrication; b) SEM images of MSC monolayer; c) SEM images of JMSC with Ni(10nm) coating by electron beam deposition.

Therefore, taking advantage of such "unwanted" aggregations "problem" during the classic synthesis of MSNPs, we propose a novel Janus mesoporous silica cluster (JMSC) based motors which are driven by bio-catalytic reaction induced bubble propulsion. Hereby, micro-sized MSC consisted of MSNPs with size less than 100 nm was fabricated (**Figure 1**). Via surface chemistry functionalization, the MSC was initially modified with carboxylic acid groups. Then, one side of the MSC was covered with magnetic metal layer (Ni) by electron-beam (E-beam) deposition, yielding JMSC. The magnetic layer (Ni) can be used for external magnetic guidance of the JMSC motors' movement.[12] Catalase enzyme was conjugated onto the uncovered side of the JMSC, to catalyse decomposition reaction of H_2O_2.[30] The rough surface with small cavities and gaps at the uncovered side of the JMSC motors can provide possible nucleation sites for O_2 bubble generation. More importantly, unlike other Janus motors by using solid spheres, the mesoporous structure of the JMSC motors have uniform nano-channels with high surface area and large pore volume, which can be used for cargos molecules loading and thus realize cargo delivery by the bio-catalytic reaction driven JMSC motors.

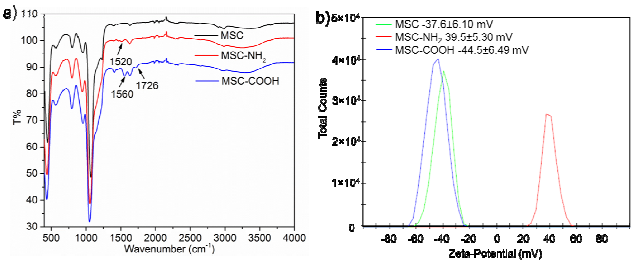

Figure 2. a) FT-IR spectra and b) Zeta-potential values of MSC, MSC-NH_2, and MSC-COOH, indicate the surface functionalization process.

MSC was fabricated by a modified sol-gel process that was used to prepare mesoporous silica nanoparticles.[20, 31, 32] Typically, silica precursor TEOS was added into an aqueous base solution containing catalyst NaOH and surfactant cetyltrimethylammonium bromide (CTAB) under vigorous stirring. After 1 h reaction, small amount of additional TEOS was added to induce more aggregation of MSNPs under mild stirring, yielding more MSC than normal conditions. Then, the MSC was suspended in EtOH solution containing (3-aminopropyl)triethoxysilane (APTES) and stirred for 24 h to produce the amino modified MSC, noted as MSC-NH_2. From the FT-IR spectra of MSC-NH_2 (red curve in figure 2a), a new peak at 1520 cm^{-1} due to primary amine appeared.[33] And zeta potential value was reversed from a negative value (-37.6±6.10 mV) of bare MSC to a positive value (39.5±5.30 mV) of MSC-NH_2. Then, the MSC-NH_2 was converted into carboxylic acid groups (-COOH) functionalized MSC, noted as MSC-COOH. Extra peaks at 1726 cm^{-1} contributed by –COOH groups were found in the FT-IR spectra of MSC-COOH. Another new peak at 1560 cm^{-1} due to amide bond proved the conjugation process between primary amine and succinic anhydride.[33-35] The zeta potential value of MSC-COOH was again reversed to a negative value (-44.5±6.49 mV), indicating successful functionalization of carboxylic acid groups on the surface of MSC-COOH.

Before E-beam deposition, a monolayer of MSC-COOH was first prepared (Figure 1a) by dipping ethanol solution containing MSC-COOH onto a clean glass slide that had been pre-treated with oxygen plasma to make it hydrophilic and ensure the good spreading of the dipped MSC-COOH solution. The prepared monolayer of MSC-COOH was observed by scanning electron microscopy (SEM) (Figure 1b). The presence of micros-sized MSCs with irregular shapes was indicated by read circles. Magnetic layer of Ni about 15 nm was deposited and the obtained JMSC with Ni coating, denoted as JMSC@Ni, was collected by sonication in DI H_2O. After E-beam deposition, the Ni coating layer was clearly observed by both SEM and transmission electron microscopy (TEM) images, as shown in figure 1b and 1c. From the SEM and TEM images, the size of MSNP that comprise the MSC was found to be around 80 nm. More importantly, the aggregation of these MSNPs produced rough surface of MSC with small cavities and gaps between MSNPs, which is critical for the bubble generation.

Afterwards, catalase enzyme was conjugated onto the non-coated side of the JMSC@Ni via 1-Ethyl-3-(3-dimethylaminopropyl)carbodiimide (EDC)/ N-Hydroxysuccinimide (NHS) chemistry. The carboxylic acid groups were first activated by stirring the JMSC@Ni in PBS buffer (pH=6.0) containing EDC/NHS for 1h. Then, catalase aqueous solution was added and the mixture solution was adjusted to slightly base condition about pH=8.5 by adding proper amount of dilute NaOH aqueous solution. After 24 h reaction, the catalase conjugated JMSC@Ni, denoted as JMSC@Ni-Catalse was collected by centrifugation and washed with DI H_2O (Figure 3a).

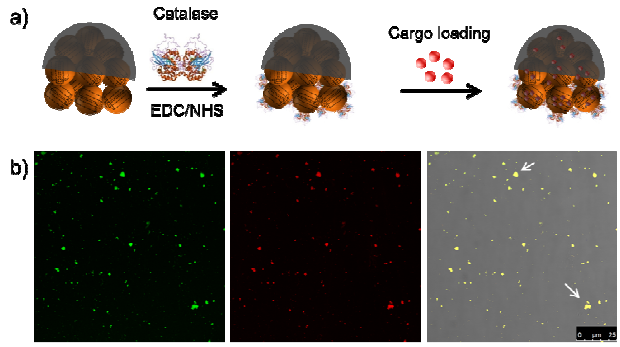

Figure 3. a) Schematic illustration of catalase conjugation on the non-coated side of JMSC and further cargo (Rh.B) loading inside the mesopores of JMSC motor. b) CLSM images of Rh.B loaded JMSC motor. From left to right are green channel (FITC), red channel (Rh.B), and overlay of the bright field, green and red channels. (scale bar=25 µm)

The cargo loading capability of the JMSC motors was tested. FITC labelled JMSC was first fabricated. Fluorescence dye Rhodamine B (Rh.B) was chosen as model cargos. The JMSC(FITC)@Ni-Catalase was suspended in Rh.B solution (0.5 mg mL^{-1}). After stirring for 24 h to ensure the cargo molecule loading into the mesopores by free diffusion, the Rh.B loaded JMSC(FITC)@-catalase was collected by centrifugation and washed with DI H_2O several times. Then, confocal laser scanning microscopy (CLSM) was used to confirm the loading of the cargo molecule inside the JMSC motors. From figure 3b, we found that red fluorescence dots due to the presence of Rh.B cargo molecules were completely overlapped with the green fluorescence dots representing locations of the FITC labelled JMSC motors, as we only find yellow dots (indicated by white arrows) in the overlay image, which certified the cargo loading inside the JMSC motor.

In order to prove the successful conjugation of catalase by EDC/NHS chemistry, as well as their catalytic activity after conjugation, the catalase conjugated JMSC was centrifuged and presented as a small pellet at the bottom of a tube. Then, one drop of H_2O_2 solution (10 µL, 30%) was added. Once the H_2O_2 solution contact the pellet at the bottom, vigorous bubble generation was observed (video S1 in the supporting information (SI)). After 24 h storage at room temperature, the same experiment was repeated. It was found that the catalytic capability of catalase remained as similar as before (Video S2 in the SI), suggesting that the bio-catalytic activity of catalase conjugated on the JMSC motors was maintained. Besides, conjugated catalase was not only reusable, but also capable of surviving relatively long time, at least up to 24 h at room temperature.

The bio-catalytic driven motion of the JMSC motor was first tested without magnetic guidance. The JMSC@Ni-catalase was suspended in an aqueous solution containing 3 wt% H_2O_2 which

was used as the fuel. Bubble generation against the movement direction was clearly observed (Video S3 in the SI), moving from the left to the right (at the up left of the video). As expected, the JMSC motor moved in a straight pathway, heading the side of Ni coating layer, while the bubble generation from the catalase conjugated side, providing the driving force for the movement by bubble propulsion mechanism.

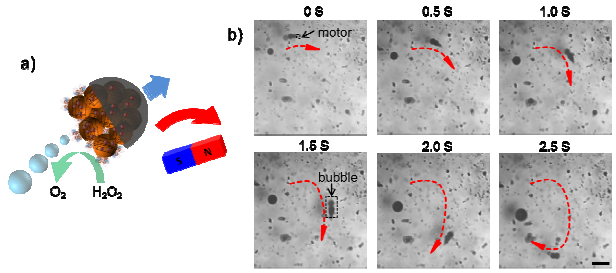

Figure 4. a) Schematic illustration and b) video snaps of bio-catalytic reaction driven motion of catalase conjugated JMSC motor under magnetic guidance with 3 wt% H_2O_2. (scale bar=200 µm)

Then, an external magnetic field was applied by using a permanent magnet, illustrated in figure 4a. Under magnetic guidance, the movement direction can be readily changed by varying the orientation of the magnetic field, as the trajectory was shown in figure 4b by the red curve. The JMSC motor indicated by the black arrow effectively produced bubbles to provide the driving force for the motor. We also observed motion of JMSC by bubble propulsion with H_2O_2 concentration as low as 1.5 wt%. The lower limit of H_2O_2 fuel concentration was found to be about 1 wt%, under which value bubble generation could barely be observed. Clearly, the JMSC motor was driven by bubble propulsion mechanism. The bubble generation should be attributed to the rough surface with small cavities at the catalytic side of the JMSC motor. However, even under the same concentration of H_2O_2, the bubble generation rate, bubble size and speed of the motors varied a lot (Video S3 and S4), which can be explained by the non-uniform size and irregular shape of the JMSC motors given by uncontrolled aggregation of MSNPs during the synthesis.

Conclusions

In summary, a bio-catalytically driven JMSC motor with remote magnetic control on motion directionality was successfully produced. Catalase enzyme was anchored onto the JMSC motor to provide driving force by decomposition of H_2O_2. Taking advantage of the rough surface with small cavities/gaps between aggregated MSNPs, O_2 bubbles were effectively generated, resulting in bubble propulsion for the JMSC motors movement. The mesoporous property of the novel motor was used for cargo loading and therefore the JMSC motor could act as an effective delivery vehicle. Magnetic coating layer (Ni) allows for remote control on the movement direction of the JMSC motor. Possibility of transporting cargo molecules to desired locations by the JMSC motor can be expected. Future research will focus on controlled self-assembly of MSNPs to produce JMSC motors with required size and shape, which will be helpful to realize stable and efficient bubble generation, as well as controlled speed of the JMSC motor.

Acknowledgement

This work is financially supported by the European Research Council under the European Union's Seventh Framework Programme (FP7/20072013)/ERC grant agreement [no. 311529], and Alexander von Humboldt Foundation. Authors thank Prof. Peter A. van Aken and Mr. Kersten Hahn for supporting in TEM imaging.

Notes and references

[a] *Max Planck Institute for Intelligent Systems, Heisenbergstraße 3, 70569 Stuttgart,Germany. E-mail: sanchez@is.mpg.de*

† Electronic Supplementary Information (ESI) available: [details of any supplementary information available should be included here]. See DOI: 10.1039/b000000x/

1. W. Gao and J. Wang, *ACS Nano*, 2014, **8**, 3170.
2. M. Guix, C. C. Mayorga-Martinez and A. Merkoçi, *Chem. Rev.*, 2014, **114**, 6285.
3. A. Brown and W. Poon, *Soft Matter*, 2014, **10**, 4016.
4. T.-C. Lee, M. Alarcón-Correa, C. Miksch, K. Hahn, J. G. Gibbs and P. Fischer, *Nano Lett.*, 2014, **14**, 2407.
5. S. Ebbens, D. A. Gregory, G. Dunderdale, J. R. Howse, Y. Ibrahim, T. B. Liverpool and R. Golestanian, *EPL (Europhysics Letters)*, 2014, **106**, 58003.
6. W. Duan, R. Liu and A. Sen, *J. Am. Chem. Soc.*, 2013, **135**, 1280.
7. W. Duan, M. Ibele, R. Liu and A. Sen, *Eur. Phys. J. E*, 2012, **35**, 1.
8. M. Manjare, B. Yang and Y. P. Zhao, *Appl. Phys. Lett.*, 2012, **109**, 128305.
9. J. G. Gibbs and Y.-P. Zhao, *Appl. Phys. Lett.*, 2009, **94**, 163104.
10. S. Wang and N. Wu, *Langmuir*, 2014, **30**, 3477.
11. S. J. Ebbens and J. R. Howse, *Langmuir*, 2011, **27**, 12293.
12. L. Baraban, D. Makarov, R. Streubel, I. Mönch, D. Grimm, S. Sanchez and O. G. Schmidt, *ACS Nano*, 2012, **6**, 3383.
13. L. Zhang and Y. Zhu, *Langmuir*, 2012, **28**, 13201.
14. N. Suzuki, X. Jiang, L. Radhakrishnan, K. Takai, K. Shimasaki, Y.-T. Huang, N. Miyamoto and Y. Yamauchi, *Bull. Chem. Soc. Jpn.*, 2011, **84**, 812.
15. P. Borah, X. Ma, K. T. Nguyen and Y. Zhao, *Angew. Chem., Int. Ed.*, 2012, **51**, 7756.
16. Q. Zhang, F. Liu, K. T. Nguyen, X. Ma, X. Wang, B. Xing and Y. Zhao, *Adv. Funct. Mater.*, 2012, **22**, 5144.
17. X. Ma, C. Teh, Q. Zhang, P. Borah, C. Choong, V. Korzh and Y. Zhao, *Antioxid Redox Signal.*, 2014, ***21***, 707.
18. K. C. W. Wu and Y. Yamauchi, *J. Mater. Chem.*, 2012, **22**, 1251.
19. Y. D. Chiang, H. Y. Lian, S. Y. Leo, S. G. Wang, Y. Yamauchi and K. C. W. Wu, *J. Phys. Chem. C*, 2011, **115**, 13158.
20. Z. Li, J. C. Barnes, A. Bosoy, J. F. Stoddart and J. I. Zink, *Chem. Soc. Rev.*, 2012, **41**, 2590.
21. M. Xuan, J. Shao, X. Lin, L. Dai and Q. He, *ChemPhysChem*, 2014, **15**, 2255.
22. Y. Mei, G. Huang, A. A. Solovev, E. B. Ureña, I. Mönch, F. Ding, T. Reindl, R. K. Y. Fu, P. K. Chu and O. G. Schmidt, *Adv. Mater.*, 2008, **20**, 4085.
23. A. A. Solovev, Y. Mei, E. Bermúdez Ureña, G. Huang and O. G. Schmidt, *Small*, 2009, **5**, 1688.
24. L. Soler, V. Magdanz, V. M. Fomin, S. Sanchez and O. G. Schmidt, *ACS Nano*, 2013, **7**, 9611.
25. S. M. Harazim, W. Xi, C. K. Schmidt, S. Sanchez and O. G. Schmidt, *J. Mater. Chem.*, 2012, **22**, 2878.
26. V. M. Fomin, M. Hippler, V. Magdanz, L. Soler, S. Sanchez and O. G. Schmidt, *Ieee T Robot*, 2014, **30**, 40.
27. B. Jurado-Sánchez, S. Sattayasamitsathit, W. Gao, L. Santos, Y. Fedorak, V. V. Singh, J. Orozco, M. Galarnyk and J. Wang, *Small*, 2014, DOI: 10.1002/smll.201402215.
28. S.-H. Wu, C.-Y. Mou and H.-P. Lin, *Chem. Soc. Rev.*, 2013, **42**, 3862.

29. Q. Zhang, X. Wang, P.-Z. Li, K. T. Nguyen, X.-J. Wang, Z. Luo, H. Zhang, N. S. Tan and Y. Zhao, *Adv. Funct. Mater.*, 2014, **24**, 2450.
30. S. Sanchez, A. A. Solovev, Y. Mei and O. G. Schmidt, *J. Am. Chem. Soc.*, 2010, **132**, 13144.
31. F. Q. Tang, L. L. Li and D. Chen, *Advanced Materials*, 2012, **24**, 1504.
32. Q. He and J. Shi, *J. Mater. Chem.*, 2011, **21**, 5845.
33. X. Ma, O. S. Ong and Y. Zhao, *Biomater. Sci.*, 2013, **1**, 912.
34. B. M. Cash, L. Wang and B. C. Benicewicz, *J. Polym. Sci. A Polym. Chem.*, 2012, **50**, 2533.
35. Y. An, M. Chen, Q. Xue and W. Liu, *J. Colloid Interf. Sci.*, 2007, **311**, 507.

TOC figure